



# Magnetically aligned nanodiscs enable direct measurement of $^{17}\text{O}$ residual quadrupolar coupling for small molecules



Samuel D. McCalpin<sup>a</sup>, Riqiang Fu<sup>b</sup>, Thirupathi Ravula<sup>a,c</sup>, Gang Wu<sup>d</sup>, Ayyalusamy Ramamoorthy<sup>a,c,\*</sup>

<sup>a</sup> Department of Chemistry, University of Michigan, Ann Arbor, MI 48109, USA

<sup>b</sup> National High Magnetic Field Laboratory, Florida State University, Tallahassee, FL 32310, USA

<sup>c</sup> Biophysics, Biomedical Engineering, Macromolecular Science and Engineering, University of Michigan, Ann Arbor, MI 48109, USA

<sup>d</sup> Department of Chemistry, Queen's University, Kingston, Ontario K7L 3N6, Canada

## ARTICLE INFO

### Article history:

Received 7 October 2022

Revised 17 November 2022

Accepted 18 November 2022

Available online 28 November 2022

### Keywords:

$^{17}\text{O}$  NMR

Residual Quadrupolar Coupling

Nanodisc

## ABSTRACT

The use of  $^{17}\text{O}$  in NMR spectroscopy for structural studies has been limited due to its low natural abundance, low gyromagnetic ratio, and quadrupolar relaxation. Previous solution  $^{17}\text{O}$  work has primarily focused on studies of liquids where the  $^{17}\text{O}$  quadrupolar coupling is averaged to zero by isotropic molecular tumbling, and therefore has ignored the structural information contained in this parameter. Here, we use magnetically aligned polymer nanodiscs as an alignment medium to measure residual quadrupolar couplings (RQCs) for  $^{17}\text{O}$ -labelled benzoic acid in the aqueous phase. We show that increasing the magnetic field strength improves spectral sensitivity and resolution and that each satellite peak of the expected pentet pattern resolves clearly at 18.8 T. We observed no significant dependence of the RQC magnitudes on the magnetic field strength. However, changing the orientation of the alignment medium alters the RQC by a consistent factor, suggesting that  $^{17}\text{O}$  RQCs measured in this way can provide reliable orientational information for elucidations of molecular structures.

© 2022 Elsevier Inc. All rights reserved.

## 1. Introduction

Oxygen is an essential component of organic and biological molecular structures, which NMR spectroscopy is uniquely positioned to directly observe. A wealth of work has established the utility of probing molecular structure using  $^{17}\text{O}$  NMR spectroscopy [1–3]. However, compared to other commonly used nuclei in NMR spectroscopy of organic molecules (hydrogen, carbon, nitrogen, phosphorus), several factors contribute to the difficulty of studying oxygen nuclei by NMR spectroscopy. First, the only NMR-active oxygen nucleus,  $^{17}\text{O}$ , has a natural abundance of only 0.037 % [4]. Second, sensitivity of  $^{17}\text{O}$  NMR is limited by its low gyromagnetic ratio (about 1/7th of that of  $^1\text{H}$ ) [1,5]. And third, because  $^{17}\text{O}$  has a nuclear spin quantum number of 5/2, it undergoes the nuclear electric quadrupolar interaction [1]. In solution, the quadrupolar interaction leads to very short transverse relaxation times ( $T_2$ ), providing a fundamental limit to spectral resolution in this phase.  $T_2$  times can be relatively long in the solid-state due to restricted molecular motions, though the quadrupolar interaction still causes substantial line broadening because quadrupolar coupling has an anisotropic dependence. Due to the second-order quadrupolar

interaction scaling inversely with the strength of the external magnetic field, high magnetic fields are desirable for NMR spectroscopy of quadrupolar nuclei. Practically, the result of these considerations is that  $^{17}\text{O}$  NMR spectroscopy has been largely restricted to studies of isotope-labelled molecules using solid-state NMR experiments conducted under high magnetic fields [1].

Nevertheless, recent improvements to experimental methodologies have demonstrated the feasibility of overcoming each challenge to using  $^{17}\text{O}$  NMR spectroscopy to study organic and biological molecules. Advances in total and site-specific  $^{17}\text{O}$ -labelling techniques based on water exchange and recombinant protein expression have reduced the experimental burden of  $^{17}\text{O}$  incorporation into organic small molecules and proteins [6–8]. Generally applicable sensitivity enhancement techniques, such as dynamic nuclear polarization (DNP) [9], ultrafast and cryogenic magic angle spinning (MAS) [10], and paramagnetic doping [7], offer powerful approaches for improving  $^{17}\text{O}$  spectral resolution and sensitivity. And lastly, the quadrupolar interaction can be at least partly avoided by employing methods which simulate isotropic conditions, such as quadrupole-central-transition (QCT) NMR and multiple-quantum MAS. Collectively, such labelling, sensitivity enhancement, and quadrupolar interaction suppression or avoidance strategies have allowed  $^{17}\text{O}$  NMR-based studies of inorganic solids at natural abundance [11], of hydrogen bonding networks

\* Corresponding author.

E-mail address: [ramamoor@umich.edu](mailto:ramamoor@umich.edu) (A. Ramamoorthy).

in carbohydrate crystals and ion channel pores [7,12], and of protein–ligand interactions in both aqueous phase and solid-state conditions [13–16].

While techniques that reduce anisotropic interactions and cause spectra to appear more isotropic can significantly improve sensitivity and resolution, they also sacrifice rich structural information. The three common anisotropic NMR parameters, dipolar couplings, quadrupolar couplings, and chemical shift anisotropies, each provide orientational and structural information based on relative orientations of their associated tensors [17–20]. Though these interactions are averaged in solution by fast isotropic motions, the development of weakly aligning media has enabled the recovery of a portion of this information as residual dipolar couplings (RDCs) or residual chemical shift anisotropies (RCSAs). Inclusion of RDCs and RCSAs as angular constraints in structure calculations of biological and small molecules is now routine [21–24]. In contrast, relatively few studies have even reported measuring residual quadrupolar couplings (RQCs) in partially aligned samples, due to the low abundance and inherent sensitivity limitations of quadrupolar nuclei [19,25]. These studies have been primarily focused on  $^2\text{H}$  RQCs with few reports for other nuclei such as  $^7\text{Li}$ ,  $^9\text{Be}$ ,  $^{14}\text{N}$ ,  $^{17}\text{O}$ ,  $^{23}\text{Na}$ , and  $^{133}\text{Cs}$ . Many were also experimentally challenging as they achieved alignment mechanically or using an external electric field [26–27]. An exciting study by Lesot et al. demonstrated the ability of  $^2\text{H}$  RQCs to unambiguously determine the correct configuration of stereogenic centers in two chiral small molecules [25]. But the reports of RQCs from other nuclei were restricted to studying non-structural or low-resolution features such as the aggregation of organolithium compounds [28], discrimination between symmetric and non-symmetric coordination states of  $^9\text{Be}$  [29], alignment of phospholipids containing  $^{14}\text{N}$  [30], and local environmental order around  $^{23}\text{Na}^+$  and  $^{133}\text{Cs}^+$  ions [31–32].

$^{17}\text{O}$  RQCs have previously been observed by us and by others for bulk water and for endofullerene-encapsulated water [33–36], but to our knowledge have never been described for a non-solvent molecule. Here, we report the measurement of  $^{17}\text{O}$  RQC for an aqueous-phase small molecule using magnetically aligned polymer nanodiscs as an alignment medium. We also describe the dependence of  $^{17}\text{O}$  RQC and NMR spectral features on magnetic field strength and orientation of the sample alignment. Polymer nanodiscs are a convenient alignment medium because in the presence of an external magnetic field and within a certain temperature range, they spontaneously align with their bilayer normals perpendicular to the magnetic field direction [37]. Additionally, the nanodisc orientation can be flipped by  $90^\circ$ , such that the bilayer normal is parallel to the magnetic field axis, with the addition of paramagnetic lanthanide ions [38]. Collectively, our data demonstrates the ease of measurement of  $^{17}\text{O}$  RQCs from aqueous small molecules and the feasibility of incorporating this information into future investigations of molecular structure and orientation.

## 2. Experimental methods and Materials

**Materials.** 1,2-dimyristoyl-*sn*-glycero-3-phosphocholine (DMPC) was purchased from Avanti Polar Lipids, SMA-EA and pentyl inulin polymers were synthesized as described previously [30,39], and all other chemicals were obtained from Sigma-Aldrich.  $^{17}\text{O}$ -labelled benzoic acid was prepared following the procedure described in a previous study [40].

**Preparation of Nanodiscs and NMR Samples.** DMPC was solubilized to 200 mg/mL in aqueous buffer (10 mM Tris, 50 mM NaCl, pH 7.4), and the DMPC liposomes were homogenized by applying five freeze/thaw cycles. A nanodisc-forming polymer, amine-modified styrene:maleic acid (SMA-EA) or pentyl inulin (INPEN)

was then added to the liposomes to achieve a 1:1 polymer:DMPC mass ratio. Homogenous nanodiscs were prepared by applying five more freeze–thaw cycles. Nanodiscs were concentrated by spin centrifugation at  $4000 \times g$  and  $4^\circ\text{C}$  using Amicon Ultra Centrifugal Filters (50 K MWCO). Excess polymer was removed by washing the nanodisc sample with at least 3 sample volumes of buffer during the centrifugation.  $^{17}\text{O}$ -benzoic acid was solubilized in one molar equivalent of NaOH and added to concentrated nanodiscs to a final concentration of 30 mM.  $\text{YbCl}_3$  was prepared as a 100 mM stock in water and added to nanodisc samples from this stock.

**9.4 T NMR Experiments.** All NMR experiments at 9.4 T were performed using a Bruker solid-state NMR spectrometer and a 5 mm HXY MAS probe (Chemagnetics), and all spectra were acquired under static conditions. The probe was tuned to 400.11 MHz for  $^1\text{H}$  nuclei, 161.97 MHz for  $^{31}\text{P}$  nuclei, and 54.23 MHz for  $^{17}\text{O}$  nuclei.  $^{31}\text{P}$  NMR spectra were acquired by taking 512 scans with a  $5 \mu\text{s}$   $90^\circ$  pulse (80 W), a 3.0 s recycle delay, and 20 W spinlock proton decoupling [41].  $^{17}\text{O}$  NMR spectra were acquired by taking 102,400 scans using a Hahn-Echo pulse sequence with a  $5 \mu\text{s}$   $90^\circ$  pulse, a 9.41  $\mu\text{s}$  echo delay, and a 50 ms recycle delay.

**14.1 T and 18.8 T NMR Experiments.** NMR experiments at 14.1 T and 18.8 T were conducted using a home-made low electrical field  $^1\text{H}$ - $^{17}\text{O}$  double-resonance probe with a 5 mm bicelle coil. The  $^{17}\text{O}$  Larmor frequencies used to tune the  $^{17}\text{O}$  channel were 81.36 MHz and 108.44 MHz on the 14.1 T and 18.8 T NMR spectrometers, respectively.  $^{17}\text{O}$  spectra were acquired using triple-pulse excitation [42] with a  $5.5 \mu\text{s}$   $90^\circ$  pulse and a 100 ms recycle delay. We collected 10,240 (without  $\text{YbCl}_3$  at 14.1 T and with  $\text{YbCl}_3$  at 18.8 T), 20,480 (without  $\text{YbCl}_3$  at 18.8 T), or 51,200 (with  $\text{YbCl}_3$  at 14.1 T) scans. Spectral widths were 250 kHz for the sample with  $\text{YbCl}_3$  at 14.1 T and 100 kHz otherwise.

**NMR Data Processing.** All NMR data were processed in the Bruker TopSpin software package.  $^{31}\text{P}$  NMR spectra were processed with 20 Hz line broadening.  $^{17}\text{O}$  NMR spectra were processed with 100 Hz line broadening (9.4 T) or 250 Hz line broadening (14.1 T and 18.8 T) for presenting the full spectra and 40 Hz (9.4 T) or 0 Hz (14.1 T and 18.8 T) line broadening for displaying the water peak RQCs. Baseline correction of the  $^{17}\text{O}$  NMR spectra was performed using cubic spline interpolation. All points for the baseline correction were defined outside the region of the spectra containing the peaks corresponding to benzoic acid and water.

## 3. Results and discussion

Nanodiscs were prepared as described previously (Fig. 1) [30,39]. Briefly, DMPC liposomes were prepared by dissolving the lipid in aqueous buffer and homogenized by several freeze/thaw cycles. An appropriate amount of the amphipathic, nonionic INPEN polymer was then added to the liposomes and more freeze/thaw cycles were performed to produce homogenous nanodiscs. Temperature-dependent  $^{31}\text{P}$  NMR spectra were collected for each nanodisc sample to assess nanodisc alignment in the magnetic field (Fig. 2). In the  $^{31}\text{P}$  NMR spectra of the INPEN nanodiscs, a single narrow peak appeared at all temperatures with the aligned anisotropic chemical shift of approximately  $-14$  ppm. Increasing the temperature slightly narrowed and shifted this peak upfield, consistent with increasing homogeneity of nanodisc alignment.

To evaluate the ability of the aligned nanodiscs to provide a sufficiently anisotropic medium for the measurement of  $^{17}\text{O}$  RQC, we added doubly  $^{17}\text{O}$ -labelled benzoic acid to preprepared nanodisc samples and collected  $^{17}\text{O}$  NMR spectra at 9.4 T and between 295 and 310 K (Fig. 3). In the presence of both INPEN nanodiscs at 295 K,  $^{17}\text{O}$ -benzoic acid gave rise to a single peak in the  $^{17}\text{O}$  NMR spectrum with a chemical shift of 265 ppm. Though there are two  $^{17}\text{O}$  atoms in the molecule, this observation is consistent with

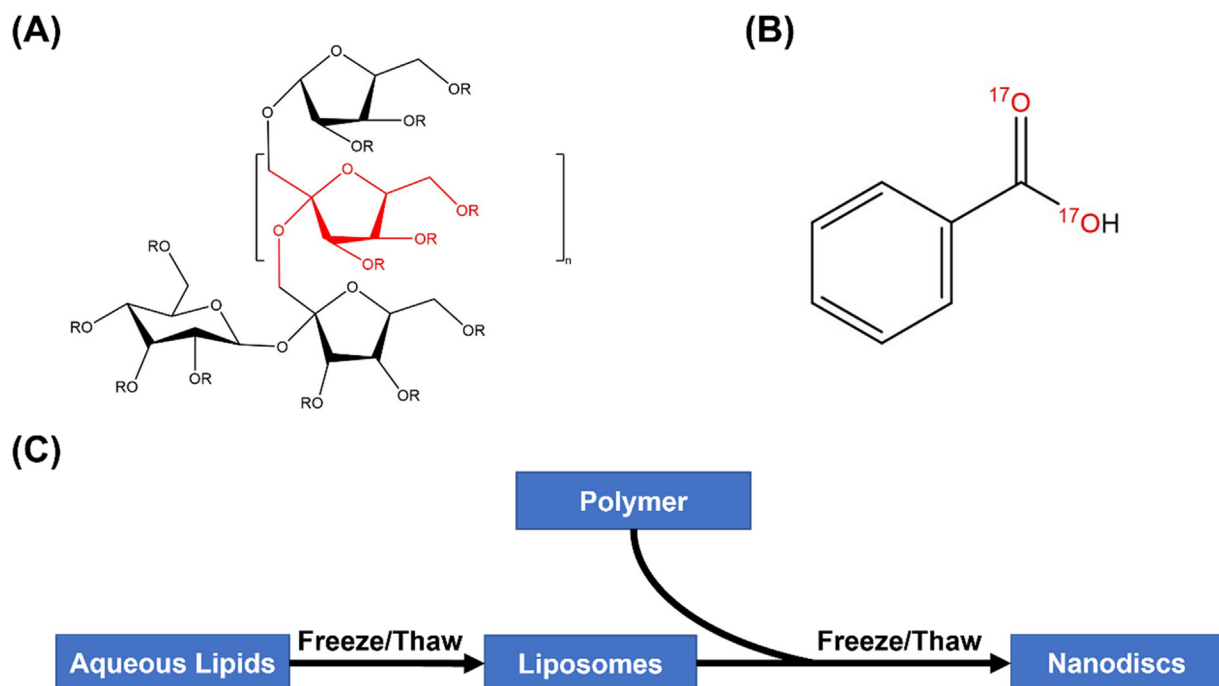


**Fig. 1.** Molecular structures of (A) INPEN and (B)  $^{17}\text{O}$ -labelled benzoic acid. (C) Schematic overview of nanodisc sample preparation. In (A) the R groups correspond to either -H or  $-(\text{CH}_2)_4\text{CH}_3$  as described in ref 39.

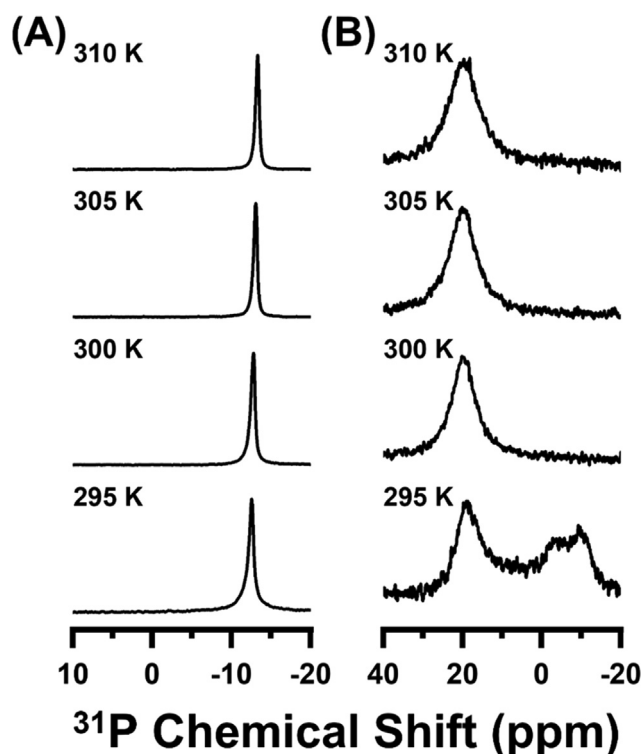


**Fig. 2.**  $^{31}\text{P}$  NMR spectra of (A) 1:1 INPEN:DMPC, 25 % w/w DMPC nanodiscs; and (B) 1:1 INPEN:DMPC, 25 % w/w DMPC nanodiscs in the presence of 4 mM  $\text{YbCl}_3$ . All samples were prepared in 10 mM Tris, 50 mM NaCl buffer and NMR spectra were collected at 9.4 T.

previous studies of  $^{17}\text{O}$ -labelled carboxylic acids in aqueous solvent and likely results from proton exchange with the solvent [43–44]. Further, this isotropic chemical shift is also consistent with that of a deprotonated carboxylic acid in the aqueous phase, as expected for benzoic acid at pH 7.4 [43]. As the temperature

increased the  $^{17}\text{O}$  NMR spectra displayed broadening and splitting of the water peak (at 0 ppm), as described previously [33], and of the benzoic acid peak. The temperature range in which this occurred corresponds exactly to the range in which the nanodiscs aligned. While quadrupolar coupling in a spin 5/2 nucleus, like  $^{17}\text{O}$ , is expected to give rise to a pentet peak pattern, resolution of the satellite peaks was low for both the water and benzoic acid signals. The first satellite peaks clearly resolved, but the outer peaks appeared only as shoulders, suggesting that the conditions of this experiment did not provide sufficient sensitivity to resolve the entire lineshape.

We repeated the same  $^{31}\text{P}$  and  $^{17}\text{O}$  NMR experiments with nanodiscs formed with the negatively charged SMA-EA polymer in place of the INPEN nanodiscs (Fig. S1). As with the previous samples, the  $^{31}\text{P}$  NMR spectra suggested alignment of the lipids and the  $^{17}\text{O}$  benzoic acid peak showed the same splitting at higher temperatures. However, the  $^{31}\text{P}$  spectra were much broader and with a shifted maximum chemical shift compared to what has been previously reported for SMA-EA nanodiscs, possibly due to poor proton decoupling, poor nanodisc formation, poor alignment in the magnetic field, or sample contamination of the polymer batch. Thus, while this data demonstrates the feasibility of observing and measuring  $^{17}\text{O}$  RQCs in different lipid-based alignment media, we hesitate to directly compare these systems here.

Clearly though, the alignment of the nanodiscs resulted in residual anisotropy which then caused the  $^{17}\text{O}$  quadrupolar interaction to appear in the NMR spectra. Defining the magnitude of the RQC as the frequency difference between peaks of the multiplet, much greater RQC was observed for benzoic acid than for water (9000 Hz vs 200 Hz, Table 1). In Table 1, we have also defined an approximate version of an order parameter as the ratio of the  $^{17}\text{O}$  RQC to the static quadrupolar coupling constant (8.0 MHz for benzoic acid and 7.6 MHz for water) [45]. Because the RQC magnitude depends on both a molecule's orientation and its order parameter, the dramatic difference in RQCs for benzoic acid and water reflects a difference in the residual orderings and/or motional restrictions experienced by the benzoic acid and the bulk water, but we cannot

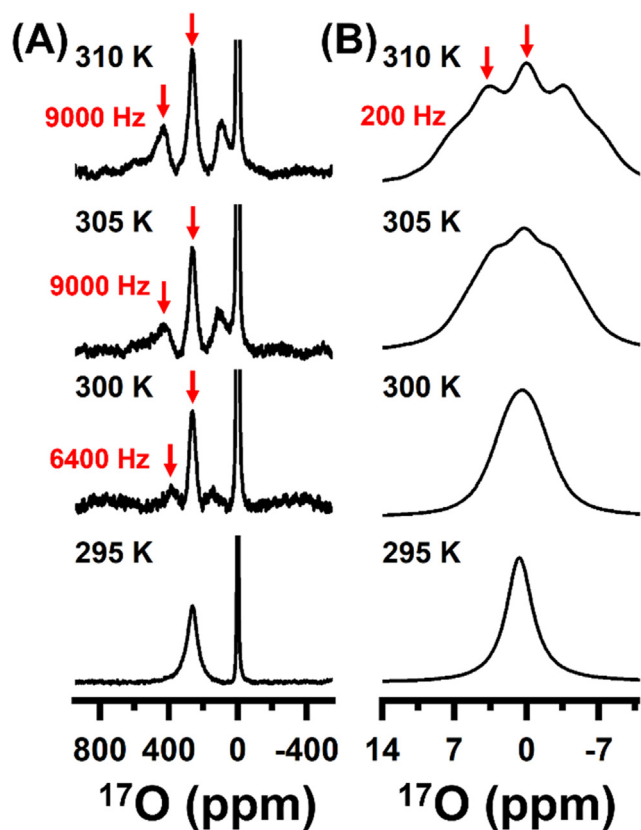


**Fig. 3.** 9.4 T  $^{17}\text{O}$  NMR spectra of 30 mM  $^{17}\text{O}$ -labelled benzoic acid in the presence of INPEN nanodiscs (details in caption of Fig. 2). RQCs for multiplets are noted in red arrows and values. The spectra in (A) display the full spectral widths, and the spectra in (B) are zoomed in to show the lineshape of the water peak.

determine the extent of each contribution based on RQCs measured in one alignment state.

It is exciting to be able to measure such a large interaction using only 1D NMR spectroscopy and magnetically aligned nanodiscs; however, accurate quantitative measurement of RQC values requires high data quality. The S/N and linewidths seen in the spectra in Fig. 2 would ideally be improved for this purpose. We expected that by using higher magnetic field strengths and an improved pulse sequence we could obtain spectra with reduced noise levels and narrower lineshapes. Accordingly, we prepared a new sample with INPEN nanodiscs as before and collected the same set of  $^{17}\text{O}$  NMR spectra at 14.1 T and 18.8 T fields and using triple pulse excitation (Fig. 4) [42]. The spectra primarily displayed the same features as observed previously with a few noticeable differences. The benzoic acid peak again split into a multiplet above 305 K, but at 14.1 T and especially at 18.8 T the outer satellite

peaks clearly resolved with narrower lines, indicating that sensitivity increases with magnetic field strength. We also note that there are slight asymmetries in the multiplet lineshapes, possibly due to  $^{17}\text{O}$  CSA-quadrupolar correlation [46–48]. Qualitatively, the asymmetries appear to increase with magnetic field strength, consistent with a CSA contribution, but they are of small magnitude, so we cannot yet confirm whether this observation is real or an artifact of data processing.

Interestingly, the magnitude of the RQC increased only slightly between the spectra collected at 14.1 T and at 18.8 T (5.8 kHz vs 6.0 kHz at 310 K). It is well established that the quadrupolar interaction, like the dipolar interaction, does not explicitly depend on the magnetic field strength [49–50]. But it has also been shown that in partially aligned systems, the alignment, and therefore the residual anisotropic interactions, scales with the square of the magnetic field [51–52]. In these cases, partial alignment of the molecule being observed was directly caused by the external magnetic field. However, the partial alignment here was achieved by fast exchange between isotropically tumbling benzoic acid molecules in the bulk solution and ordered benzoic acid molecules in the vicinity of aligned nanodiscs. In this case, the external magnetic field primarily aligned the nanodiscs and thus only indirectly aligned the benzoic acid. Though the orientation energy of phospholipid bilayers also scales with the square of the magnetic field, there is not necessarily a direct relationship between the nanodisc orientation energy and the order parameters of benzoic acid and water [53]. In fact, we have previously shown that  $^2\text{H}$  RQCs for water in the presence of magnetically aligned SMA-QA polymer nanodiscs only slightly increased (by  $\sim 10\%$ ) between 11.7 T and 18.8 T fields [54]. Another study measured  $^2\text{H}$  RQCs from water and  $^{13}\text{C}$ - $^1\text{H}$  RDCs from a disaccharide in the presence of magnetically aligned phospholipid bicelles and found that both the RQCs and RDCs either did not significantly change or slightly decreased with increasing magnetic field strengths [55]. The authors rationalized this observation by noting that the alignment medium created two populations for both the water and aqueous disaccharide – an ordered population transiently interacting with the aligned bilayers and a disordered population tumbling isotropically in the bulk solvent – and by postulating that exchange between the two populations, which gave rise to the RQCs and RDCs, slowed at higher fields. These results would also explain some of the increase in the RQCs measured at 9.4 T versus at 14.1 T and at 18.8 T, though that sample was prepared separately, so small differences in lipid concentration likely also contributed. Regardless, our results are consistent with previous reports.

A useful property of nanodiscs as an alignment medium is that the orientation of the nanodiscs can be flipped by  $90^\circ$  by the addition of paramagnetic lanthanide ions. For structure calculations, collecting anisotropic NMR data under multiple alignment conditions improves the refinement of the alignment tensor and therefore the accuracy of the structure. To investigate the effect of flipping the nanodisc orientation on  $^{17}\text{O}$  RQCs in benzoic acid, we

**Table 1**  
Experimental Anisotropic  $^{17}\text{O}$  NMR Parameters.

Field Strength (T)	Polymer	[Yb $^{3+}$ ] (mM)	$\Delta\nu_{\text{ba}}$ (Hz) <sup>a,c</sup>	$S_{\text{ba}}$ ( $\times 10^{-4}$ ) <sup>b,c</sup>	$\Delta\nu_{\text{w}}$ (Hz) <sup>a,d</sup>	$S_{\text{w}}$ ( $\times 10^{-4}$ ) <sup>b,d</sup>
9.4	INPEN	0	9000	11	200	0.26
14.1	INPEN	0	5800	7.3	180	0.24
		4	–	–	–	–
18.8	INPEN	0	6000	7.5	190	0.25
		4	7800	9.8	195	0.26

<sup>a</sup> RQC values were approximated as the average frequency difference between peaks of the  $^{17}\text{O}$  multiplets.

<sup>b</sup> order parameters were defined here as the ratio between the measured RQC and the static quadrupolar coupling constant - from ref. 43 for both a general benzoate and liquid water.

<sup>c</sup> benzoic acid.

<sup>d</sup> water.

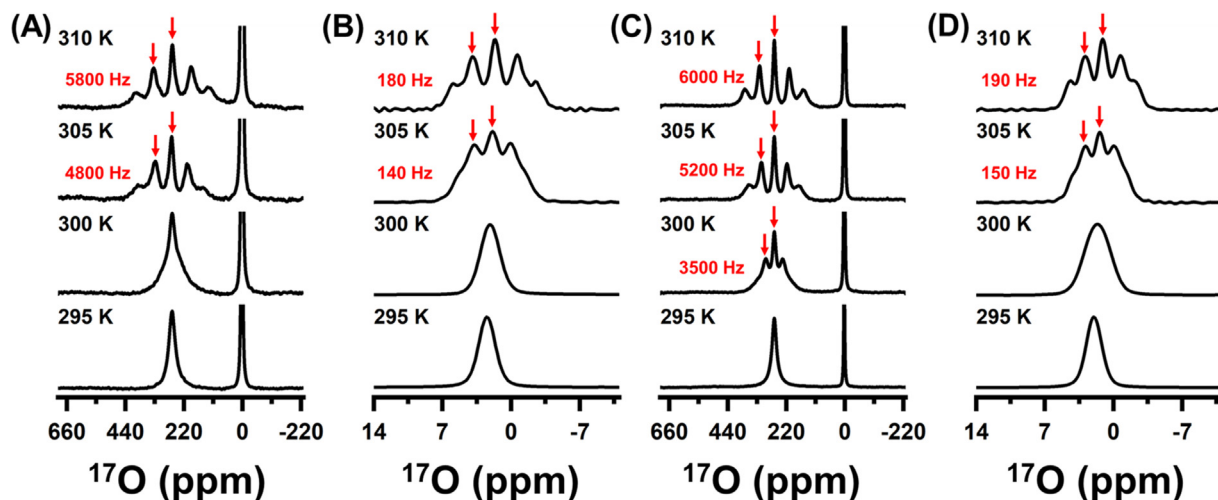


**Fig. 4.**  $^{17}\text{O}$  NMR spectra of 30 mM benzoic acid with 1:1 INPEN:DMPC, 25 % DMPC nanodiscs collected at (A, B) 14.1 T and (C, D) 18.8 T. The spectra in (A, C) display the full spectral widths, and the spectra in (B, D) are zoomed in to show the lineshape of the water peak.

prepared INPEN nanodiscs as previously and added 4 mM  $\text{YbCl}_3$ . Temperature-dependent  $^{31}\text{P}$  NMR spectra (Fig. 2) showed that the DMPC  $^{31}\text{P}$  peak shifted from  $-14$  ppm to 20 ppm upon the addition of  $\text{Yb}^{3+}$ , consistent with a flipped nanodisc orientation, and significantly broadened due to paramagnetic relaxation effects. Then we added  $^{17}\text{O}$ -benzoic acid and collected the same set of  $^{17}\text{O}$  NMR spectra at 14.1 T and 18.8 T (Fig. 5). At 14.1 T  $^{17}\text{O}$  RQC seems to have been suppressed when the nanodiscs were flipped. The isotropic peaks broadened at higher temperature for both water and benzoic acid but were asymmetric, and clear satellite peaks were not present. In contrast, at 18.8 T the expected pentet appeared above 305 K, albeit with broader lines and higher S/N compared to the original aligned sample at 18.8 T. Qualitatively, this is similar to the  $\text{Yb}^{3+}$ -induced broadening of the  $^{31}\text{P}$  spectral lines (Fig. 2), though much smaller in magnitude ( $\sim 20$  % increase in  $^{17}\text{O}$  linewidth compared to  $\sim 900$  % increase in  $^{31}\text{P}$  linewidth for samples doped with 4 mM  $\text{YbCl}_3$ ). This observation is likely due to the ordered benzoic acid molecules being in equilibrium with fast and randomly tumbling benzoic acid molecules in the

bulk water. It is possible that the paramagnetic lanthanide ions disrupted RQC at the weaker magnetic field, for example by affecting the  $^{17}\text{O}$  relaxation properties. But more research is needed to precisely determine whether the lanthanide ions have a direct effect on the RQC or an indirect effect, such as by disrupting the strength or homogeneity of the nanodisc alignment. Still, at 18.8 T the benzoic acid  $^{17}\text{O}$  RQC pentet resolved nicely, allowing measurement of the RQC magnitude. For each temperature between 300 K and 310 K, the measured RQC for  $^{17}\text{O}$ -benzoic acid is increased for the sample with the flipped alignment (bilayer normal parallel to the magnetic field axis) compared to the original aligned orientation (bilayer normal perpendicular to magnetic field axis) and the increase is consistently by a factor of  $\sim 1.3$ . Because RQCs are proportional to  $[3\cos^2\theta - 1]$  [19], the fact that the RQC increased by a consistent factor upon changing the sample alignment indicates that measuring the  $^{17}\text{O}$  RQC under different alignment conditions should in principle be useful for determining the relative orientations of the quadrupolar coupling tensor and the alignment tensor

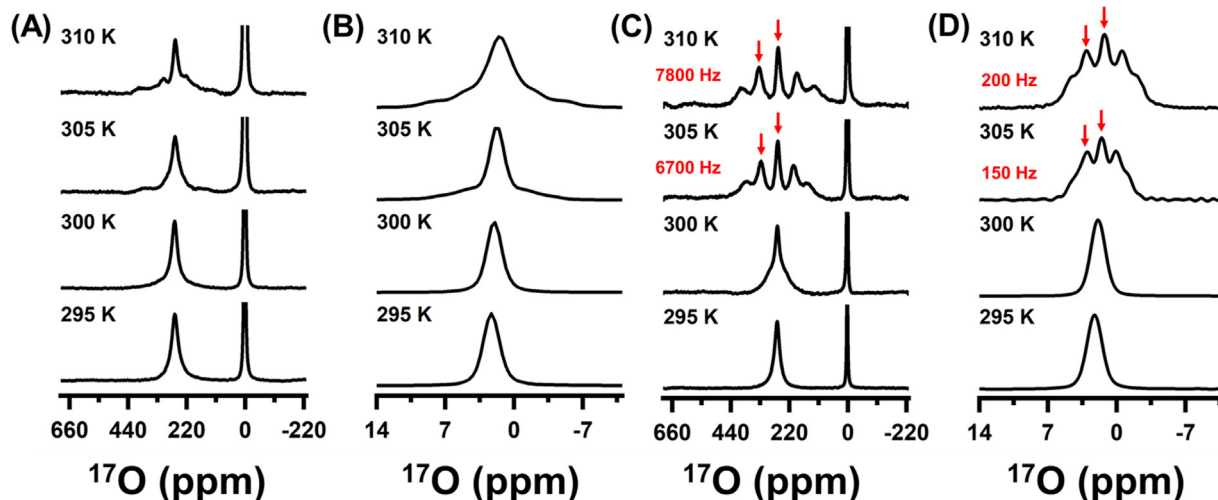


**Fig. 5.**  $^{17}\text{O}$  NMR spectra of 30 mM benzoic acid with 1:1 INPEN:DMPC, 25 % DMPC nanodiscs and 4 mM  $\text{YbCl}_3$  collected at (A, B) 14.1 T and (C, D) 18.8 T. The spectra in (A, C) display the full spectral widths, and the spectra in (B, D) are zoomed in to show the lineshape of the water peak.

#### 4. Conclusions

In summary, we have demonstrated that magnetically aligned lipid nanodiscs can be used as an alignment medium for the measurement of  $^{17}\text{O}$  RQC in an  $^{17}\text{O}$ -labelled small molecule in the aqueous phase. RQCs of several kHz in magnitude were measured using simple 1D NMR experiments and only required changing the temperature to switch between isotropic and anisotropic sample conditions. The reported results demonstrate that high magnetic field strengths are beneficial for the  $^{17}\text{O}$  experiments, namely in improving sensitivity and resolution of multiplet peaks. Lastly, the orientation of the nanodisc alignment was flipped by  $90^\circ$  before adding lanthanide ions to show that the  $^{17}\text{O}$  RQCs reliably changed in magnitude based on the nanodisc orientation. The orientation dependence of the  $^{17}\text{O}$  RQCs did not follow the expected behavior for the orientation change of the nanodiscs and therefore should provide information on the relative orientations of the  $^{17}\text{O}$  quadrupolar coupling tensor and the overall alignment tensor. However, additional work is needed to determine the signs of  $^{17}\text{O}$  RQCs and to incorporate them in molecular structure calculations. We also believe that the procedure reported here would be of use in studying molecules, such as hydrophobic drug molecules or integral membrane proteins, bound to or buried within the nanodisc lipid bilayer. In principle, measuring  $^{17}\text{O}$  RQCs at two orientations, as described here, should allow a calculation of the orientation between the  $^{17}\text{O}$  quadrupolar coupling tensor and the bilayer surface and hence the orientation of the molecule within the lipid bilayer. It might additionally be interesting to use RQCs to compare ordering of populations of the same molecule in different environments, such as bulk water versus water confined to a transmembrane protein channel. We also expect that this procedure should be generally applicable for measuring RQC in other quadrupolar nuclei, such as  $^{23}\text{Na}$ ,  $^{35}\text{Cl}$ ,  $^{39}\text{K}$ ,  $^{79}\text{Br}$ , and others.

#### Data availability

Data will be made available on request.

#### Declaration of Competing Interest

The authors declare the following financial interests/personal relationships which may be considered as potential competing interests: [Ayyalusamy Ramamoorthy has an US patent pending.].

#### Acknowledgments

This study was conducted with funding from the NIH (Grant R35GM139573 and DK13221401 to AR). The NMR experiments on the 600 and 18.8 T were carried out at the National High Magnetic Field Lab (NHMFL) supported by the NSF Cooperative Agreement DMR-1644779 and the State of Florida. GW thanks the NSERC of Canada for a discovery grant.

#### Appendix A. Supplementary material

Supplementary data to this article can be found online at <https://doi.org/10.1016/j.jmr.2022.107341>.

#### References

[1] G. Wu,  $^{17}\text{O}$  NMR studies of organic and biological molecules in aqueous solution and in the solid state, *Prog. Nucl. Magn. Reson. Spectrosc.* 114–115 (2019) 135–191, <https://doi.org/10.1016/j.pnmrs.2019.06.002>.

[2] G. Wu, Solid-State  $^{17}\text{O}$  NMR studies of organic and biological molecules: recent advances and future directions, *Solid State Nucl. Magn. Reson.* 73 (2016) 1–14, <https://doi.org/10.1016/j.ssnmr.2015.11.001>.

[3] S. Muniyappan, Y. Lin, Y.-H. Lee, J.H. Kim,  $^{17}\text{O}$  NMR spectroscopy: a novel probe for characterizing protein structure and folding, *Biology* 10 (6) (2021) 453, <https://doi.org/10.3390/biology10060453>.

[4] V. Lemaître, M.E. Smith, A. Watts, A review of oxygen-17 Solid-State NMR of organic materials—towards biological applications, *Solid State Nucl. Magn. Reson.* 26 (3) (2004) 215–235, <https://doi.org/10.1016/j.ssnmr.2004.04.004>.

[5] E. Brun, B. Derighetti, E.E. Hundt, H.H. Niebuhr, NMR of  $^{17}\text{O}$  in ruby with dynamic polarization techniques, *Phys. Lett. A* 31 (8) (1970) 416–417, [https://doi.org/10.1016/0375-9601\(70\)90371-3](https://doi.org/10.1016/0375-9601(70)90371-3).

[6] B. Lin, I. Hung, Z. Gan, P.-H. Chien, H.L. Spencer, S.P. Smith, G. Wu,  $^{17}\text{O}$  NMR studies of yeast ubiquitin in aqueous solution and in the solid state, *ChemBioChem* 22 (5) (2021) 826–829, <https://doi.org/10.1002/cbic.202000659>.

[7] J. Shen, V. Terskikh, J. Struppe, A. Hassan, M. Monette, I. Hung, Z. Gan, A. Brinkmann, G. Wu, Solid-State  $^{17}\text{O}$  NMR study of  $\alpha$ -D-glucose: exploring new frontiers in isotopic labeling, sensitivity enhancement, and NMR crystallography, *Chem. Sci.* 13 (9) (2022) 2591–2603, <https://doi.org/10.1039/D1SC06060K>.

[8] I. Hung, E.G. Keeler, W. Mao, P.L. Gorkov, R.G. Griffin, Z. Gan, Residue-Specific high-resolution  $^{17}\text{O}$  solid-state nuclear magnetic resonance of peptides: multidimensional indirect  $^1\text{H}$  detection and magic-angle spinning, *J. Phys. Chem. Lett.* 13 (28) (2022) 6549–6558, <https://doi.org/10.1021/acs.jpcclett.2c01777>.

[9] V.K. Michaelis, E. Markhasin, E. Daviso, J. Herzfeld, R.G. Griffin, Dynamic nuclear polarization of oxygen-17, *J. Phys. Chem. Lett.* 3 (15) (2012) 2030–2034, <https://doi.org/10.1021/jz2300742w>.

[10] A. Hassan, C.M. Quinn, J. Struppe, I.V. Sergeev, C. Zhang, C. Guo, B. Runge, T. Theint, H.H. Dao, C.P. Jaromic, M. Berbon, A. Lends, B. Habenstein, A. Loquet, R. Kuemmerle, B. Perrone, A.M. Gronenborn, T. Polenova, Sensitivity boosts by the CPMAS cryoprobe for challenging biological assemblies, *J. Magn. Reson.* 311 (2020), <https://doi.org/10.1016/j.jmr.2019.106680>.

[11] F. Blanc, L. Sperrin, D.A. Jefferson, S. Pawsey, M. Rosay, C.P. Grey, Dynamic nuclear polarization enhanced natural abundance  $^{17}\text{O}$  spectroscopy, *J. Am. Chem. Soc.* 135 (8) (2013) 2975–2978, <https://doi.org/10.1021/ja4004377>.

[12] J. Paulino, M. Yi, I. Hung, Z. Gan, X. Wang, E.Y. Chekmenev, H.-X. Zhou, T.A. Cross, Functional stability of water wire-carbonyl interactions in an ion channel, *Proc. Natl. Acad. Sci.* 117 (22) (2020) 11908–11915, <https://doi.org/10.1073/pnas.2001083117>.

[13] J. Zhu, E. Ye, V. Terskikh, G. Wu, Solid-State  $^{17}\text{O}$  NMR spectroscopy of large protein-ligand complexes, *Angew. Chem. Int. Ed.* 49 (45) (2010) 8399–8402, <https://doi.org/10.1002/anie.201002041>.

[14] J. Zhu, I.C.M. Kwan, G. Wu, Quadrupole-Central-Transition  $^{17}\text{O}$  NMR spectroscopy of protein–ligand complexes in solution, *J. Am. Chem. Soc.* 131 (40) (2009) 14206–14207, <https://doi.org/10.1021/ja906881n>.

[15] A.W. Tang, X. Kong, V. Terskikh, G. Wu, Solid-State  $^{17}\text{O}$  NMR of unstable acyl-enzyme intermediates: a direct probe of hydrogen bonding interactions in the oxyanion hole of serine proteases, *J. Phys. Chem. B* 120 (43) (2016) 11142–11150, <https://doi.org/10.1021/acs.jpcc.6b08798>.

[16] H.C. Lee, E. Oldfield, Oxygen-17 nuclear magnetic resonance-spectroscopic studies of carbonmonoxy hemoproteins, *J. Am. Chem. Soc.* 111 (5) (1989) 1584–1590, <https://doi.org/10.1021/ja00187a009>.

[17] Y. Liu, J. Saurí, E. Mevers, M.W. Peczu, H. Hiemstra, J. Clardy, G.E. Martin, R.T. Williamson, Unequivocal determination of complex molecular structures using anisotropic NMR measurements, *Science* 356 (6333) (2017) eaam5349, <https://doi.org/10.1126/science.aam5349>.

[18] Y. Liu, A. Navarro-Vázquez, R.R. Gil, C. Griesinger, G.E. Martin, R.T. Williamson, Application of anisotropic NMR parameters to the confirmation of molecular structure, *Nat. Protoc.* 14 (1) (2019) 217–247, <https://doi.org/10.1038/s41596-018-0091-9>.

[19] A. Navarro-Vázquez, P. Berdagué, P. Lesot, Integrated computational protocol for the analysis of quadrupolar splittings from natural-abundance deuterium NMR spectra in (Chiral) oriented media, *ChemPhysChem* 18 (10) (2017) 1252–1266, <https://doi.org/10.1002/cphc.201601423>.

[20] A. Navarro-Vázquez, R.R. Gil, K. Blinov, Computer-Assisted 3D Structure Elucidation (CASE-3D) of natural products combining isotropic and anisotropic NMR parameters, *J. Nat. Prod.* 81 (1) (2018) 203–210, <https://doi.org/10.1021/acs.jnatprod.7b00926>.

[21] J.H. Prestegard, C.M. Bougault, A.I. Kishore, Residual Dipolar Couplings in Structure Determination of Biomolecules, *Chem. Rev.* 104 (8) (2004) 3519–3540, <https://doi.org/10.1021/cr030419i>.

[22] G. Kummerlöwe, B. Luy, Residual dipolar couplings as a tool in determining the structure of organic molecules, *TrAC Trends Anal. Chem.* 28 (4) (2009) 483–493, <https://doi.org/10.1016/j.trac.2008.11.016>.

[23] K. Chen, N. Tjandra, The use of residual dipolar coupling in studying proteins by NMR, *Top. Curr. Chem.* 326 (2012) 47–67, [https://doi.org/10.1007/128\\_2011\\_215](https://doi.org/10.1007/128_2011_215).

[24] F. Hallwass, M. Schmidt, H. Sun, A. Mazur, G. Kummerlöwe, B. Luy, A. Navarro-Vázquez, C. Griesinger, U.M. Reinscheid, Residual Chemical Shift Anisotropy (RCSA): a tool for the analysis of the configuration of small molecules, *Angew. Chem. Int. Ed.* 50 (40) (2011) 9487–9490, <https://doi.org/10.1002/anie.201101784>.

- [25] P. Lesot, R.R. Gil, P. Berdagué, A. Navarro-Vázquez, Deuterium residual quadrupolar couplings: crossing the current frontiers in the relative configuration analysis of natural products, *J. Nat. Prod.* 83 (10) (2020) 3141–3148, <https://doi.org/10.1021/acs.jnatprod.0c00745>.
- [26] B.H. Ruessink, C. MacLean, Electric Field Nuclear Magnetic Resonance (Application to Nuclear Quadrupole Coupling), *Z. Naturforsch* 41 (1–2) (1986) 421–424, <https://doi.org/10.1515/zna-1986-1-282>.
- [27] B.H. Ruessink, C. MacLean, The first oxygen-17 N.M.R. Spectrum of a polar liquid aligned by an electric field, *Mol. Phys.* 53 (2) (1984) 421–428, <https://doi.org/10.1080/00268978400102411>.
- [28] A.-C. Pöppler, H. Keil, D. Stalke, M. John, <sup>7</sup>Li residual quadrupolar couplings as a powerful tool to identify the degree of organolithium aggregation, *Angew. Chem. Int. Ed.* 51 (31) (2012) 7843–7846, <https://doi.org/10.1002/anie.201202116>.
- [29] K. Romanenko, J.S. Elliott, A.A. Shubin, W.P. Kuchel, Identification of Beryllium Fluoride Complexes in Mechanically Distorted Gels Using Quadrupolar Split <sup>9</sup>Be NMR Spectra Resolved with Solution-State Selective Cross-Polarization, *Phys. Chem. Chem. Phys.* 23 (31) (2021) 16932–16941, <https://doi.org/10.1039/D1CP02515E>.
- [30] T. Ravula, S.K. Ramadugu, G. Di Mauro, A. Ramamoorthy, Bioinspired, Size-Tunable Self-Assembly of Polymer-Lipid Bilayer Nanodiscs, *Angew. Chem.* 129 (38) (2017) 11624–11628, <https://doi.org/10.1002/ange.201705569>.
- [31] P.W. Kuchel, B.E. Chapman, N. Müller, W.A. Bubb, D.J. Philp, A.M. Torres, Apparatus for Rapid Adjustment of the Degree of Alignment of NMR Samples in Aqueous Media: Verification with Residual Quadrupolar Splittings in <sup>23</sup>Na and <sup>133</sup>Cs Spectra, *J. Magn. Reson.* 180 (2) (2006) 256–265, <https://doi.org/10.1016/j.jmr.2006.03.002>.
- [32] R. Kemp-Harper, S.P. Brown, C.E. Hughes, P. Styles, S. Wimperis, <sup>23</sup>Na NMR Methods for Selective Observation of Sodium Ions in Ordered Environments, *Prog. Nucl. Magn. Reson. Spectrosc.* 30 (3) (1997) 157–181, [https://doi.org/10.1016/S0079-6565\(97\)00001-0](https://doi.org/10.1016/S0079-6565(97)00001-0).
- [33] T. Ravula, B.R. Sahoo, X. Dai, A. Ramamoorthy, Natural-Abundance <sup>17</sup>O NMR Spectroscopy of Magnetically Aligned Lipid Nanodiscs, *Chem. Commun.* 56 (69) (2020) 9998–10001, <https://doi.org/10.1039/D0CC04011H>.
- [34] R. Zhang, T.A. Cross, X. Peng, R. Fu, Surprising Rigidity of Functionally Important Water Molecules Buried in the Lipid Headgroup Region, *J. Am. Chem. Soc.* 144 (17) (2022) 7881–7888, <https://doi.org/10.1021/jacs.2c02145>.
- [35] M.R. Hakala, T.C. Wong, Phase Structure and the Orientational Order of Water in the Lyotropic Mesophase of the Hexadecyltriethylammonium Bromide-Water-Pentanol System by Deuterium and Oxygen-17 Nuclear Magnetic Resonance, *Langmuir* 2 (1) (1986) 83–89, <https://doi.org/10.1021/la00067a015>.
- [36] K. Kouřil, B. Meier, S. Alom, R.J. Whitby, M.H. Levitt, Alignment of <sup>17</sup>O-Enriched Water-Endofullerene H<sub>2</sub>O@C<sub>60</sub> in a Liquid Crystal Matrix, *Faraday Discuss.* 212 (2018) 517–532, <https://doi.org/10.1039/C8FD00095F>.
- [37] T. Ravula, N.Z. Hardin, A. Ramamoorthy, Polymer Nanodiscs: Advantages and Limitations, *Chem. Phys. Lipids* 219 (2019) 45–49, <https://doi.org/10.1016/j.chemphyslip.2019.01.010>.
- [38] T. Ravula, J. Kim, D.-K. Lee, A. Ramamoorthy, Magnetic Alignment of Polymer Nanodiscs Probed by Solid-State NMR Spectroscopy, *Langmuir* 36 (5) (2020) 1258–1265, <https://doi.org/10.1021/acs.langmuir.9b03538>.
- [39] T. Ravula, A. Ramamoorthy, Synthesis, Characterization, and Nanodisc Formation of Non-Ionic Polymers\*\*, *Angew. Chem.* 133 (31) (2021) 17022–17025, <https://doi.org/10.1002/ange.202101950>.
- [40] S. Dong, K. Yamada, G. Wu, Oxygen-17 Nuclear Magnetic Resonance of Organic Solids, *Z. Naturforsch* 55 (1–2) (2000) 21–28, <https://doi.org/10.1515/zna-2000-1-205>.
- [41] B.M. Fung, A.K. Khitrin, K. Ermolaev, An Improved Broadband Decoupling Sequence for Liquid Crystals and Solids, *J. Magn. Reson.* 142 (1) (2000) 97–101, <https://doi.org/10.1006/jmre.1999.1896>.
- [42] F. Wang, S.K. Ramakrishna, P. Sun, R. Fu, Triple-Pulse Excitation: An Efficient Way for Suppressing Background Signals and Eliminating Radio-Frequency Acoustic Ringing in Direct Polarization NMR Experiments, *J. Magn. Reson.* 332 (2021), <https://doi.org/10.1016/j.jmr.2021.107067>.
- [43] I.P. Gerotheranassis, R.N. Hunston, J. Lauterwein, <sup>17</sup>O NMR Chemical Shifts of the Twenty Protein Amino Acids in Aqueous Solution, *Magn. Reson. Chem.* 23 (8) (1985) 659–665, <https://doi.org/10.1002/mrc.1260230812>.
- [44] I.P. Gerotheranassis, R. Hunston, J. Lauterwein, <sup>17</sup>O-NMR. of Enriched Acetic Acid, Glycine, Glutamic Acid and Aspartic Acid in Aqueous Solution. I. Chemical Shift Studies, *Helv. Chim. Acta* 65 (6) (1982) 1764–1773, <https://doi.org/10.1002/hlca.19820650612>.
- [45] G. Wu, Solid-State <sup>17</sup>O NMR Studies of Organic and Biological Molecules, *Prog. Nucl. Magn. Reson. Spectrosc.* 52 (2) (2008) 118–169, <https://doi.org/10.1016/j.pnmrs.2007.07.004>.
- [46] A. Kumar, C.R. Grace, P.K. Madhu, Cross-Correlations in NMR, *Prog. Nucl. Magn. Reson. Spectrosc.* 37 (3) (2000) 191–319, [https://doi.org/10.1016/S0079-6565\(00\)00023-6](https://doi.org/10.1016/S0079-6565(00)00023-6).
- [47] D.K. Lee, J.S. Santos, A. Ramamoorthy, Application of One-Dimensional Dipolar Shift Solid-State NMR Spectroscopy To Study the Backbone Conformation of Membrane-Associated Peptides in Phospholipid Bilayers, *J. Phys. Chem. B* 103 (39) (1999) 8383–8390, <https://doi.org/10.1021/jp9914929>.
- [48] R. Sarkar, D.C. Rodriguez Camargo, G. Pintacuda, B. Reif, Restoring Resolution in Biological Solid-State NMR under Conditions of Off-Magic-Angle Spinning, *J. Phys. Chem. Lett.* 6 (24) (2015) 5040–5044, <https://doi.org/10.1021/acs.jpcclett.5b02467>.
- [49] J.R. Tolman, J.M. Flanagan, M.A. Kennedy, J.H. Prestegard, Nuclear Magnetic Dipole Interactions in Field-Oriented Proteins: Information for Structure Determination in Solution, *Proc. Natl. Acad. Sci.* 92 (20) (1995) 9279–9283, <https://doi.org/10.1073/pnas.92.20.9279>.
- [50] P. Lesot, C. Aroulanda, P. Berdagué, A. Meddour, D. Merlet, J. Farjon, N. Giraud, O. Lafon, Multinuclear NMR in Polypeptide Liquid Crystals: Three Fertile Decades of Methodological Developments and Analytical Challenges, *Prog. Nucl. Magn. Reson. Spectrosc.* 116 (2020) 85–154, <https://doi.org/10.1016/j.pnmrs.2019.10.001>.
- [51] A.A. Bothner-By, C. Gayathri, P.C.M. van Zijl, C. MacLean, J.-J. Lai, K.M. Smith, High-Field Orientation Effects in the High-Resolution Proton NMR Spectra of Diverse Porphyrins, *Magn. Reson. Chem.* 23 (11) (1985) 935–938, <https://doi.org/10.1002/mrc.1260231111>.
- [52] P.C.M. van Zijl, C. MacLean, C. Skoglund, A.A. Bothner-By, NMR of Molecules Partially Oriented in the Gas Phase, *J. Magn. Reson.* 65 (2) (1969 1985.) 316–325, [https://doi.org/10.1016/0022-2364\(85\)90012-5](https://doi.org/10.1016/0022-2364(85)90012-5).
- [53] A. Naito, T. Nagao, M. Obata, Y. Shindo, M. Okamoto, S. Yokoyama, S. Tuzi, H. Saitō, Dynorphin Induced Magnetic Ordering in Lipid Bilayers as Studied by <sup>31</sup>P NMR Spectroscopy, *Biochim. Biophys. Acta BBA - Biomembr.* 1558 (1) (2002) 34–44, [https://doi.org/10.1016/S0005-2736\(01\)00420-5](https://doi.org/10.1016/S0005-2736(01)00420-5).
- [54] T. Ravula, A. Ramamoorthy, Magnetic Alignment of Polymer Macro-Nanodiscs Enables Residual-Dipolar-Coupling-Based High-Resolution Structural Studies by NMR Spectroscopy, *Angew. Chem.* 131 (42) (2019) 15067–15070, <https://doi.org/10.1002/ange.201907655>.
- [55] K. Fehér, S. Berger, Magnetic Field Dependence of Residual Dipolar Couplings Measured in Dilute Liquid Crystalline Media, *J. Magn. Reson.* 170 (2) (2004) 191–198, <https://doi.org/10.1016/j.jmr.2004.06.014>.